

algebraic (commutation) properties needed to give a representation of rotations.

The spin factor is, by Eqs. (A6) and (A8),

$$1 + \frac{1}{2}\delta\varphi[l(-i\sigma_x) + m(-i\sigma_y) + n(-i\sigma_z)], \quad (\text{A9})$$

where l, m, n are the components of the unit vector \mathbf{n} . The square of the quantity in square brackets is -1 . As is well known, iteration of the operator (A9) by

raising it to the power $\varphi/(\delta\varphi)$, with $\delta\varphi \rightarrow 0$, gives for rotation through the angle φ the operator

$$\cos(\varphi/2) + \sin(\varphi/2) \times [l(-i\sigma_x) + m(-i\sigma_y) + n(-i\sigma_z)]. \quad (\text{A10})$$

With the isomorphism (A5), this gives the quaternion operator of Eq. (5).

Theory of Inelastic Scattering of Cold Neutrons from Liquid Helium

MICHAEL COHEN* AND RICHARD P. FEYNMAN
California Institute of Technology, Pasadena, California
 (Received March 25, 1957)

A measurement of the energy losses of monoenergetic neutrons scattered from liquid He II would permit a determination of the energy-*versus*-momentum relation for the elementary excitations (phonons and rotons) in the liquid. A major part of the scattering at a fixed angle arises from production or annihilation of a single excitation and appears as sharp lines in the energy spectrum. From the position of these lines the energy-*versus*-momentum relation of the excitations can be inferred. Other processes, such as production or annihilation of multiple excitations, contribute a continuous background, and occur at a negligible rate if the incident neutrons are slow ($\lambda \gtrsim 4\text{\AA}$) and the helium cold ($T < 2^\circ\text{K}$). The total cross-section data can be accounted for by production of single excitations; the theoretical cross section, computed from a wave function previously proposed to represent excitations, agrees with experiment over the entire energy range, within 30%. Line widths in the discrete spectrum are negligible at 1°K because of the long lifetime of phonons and rotons.

I. INTRODUCTION

THE possibility of a direct experimental determination of the energy-*versus*-momentum relation for phonons in a solid was pointed out by Placzek and Van Hove.¹ They proposed to study the energy distribution of very slow neutrons scattered inelastically and coherently from the solid; if the incident neutron beam is monochromatic and if the scattering process involves only the production or annihilation of a single phonon, energy and momentum conservation imply that the neutrons emerging at a given angle can have only certain discrete energies. The energy-momentum relation for the phonons can be inferred from the angular variation of this discrete spectrum. Other processes, such as multiple phonon production or annihilation, contribute a continuous background above which the discrete spectrum is still observable.

The purpose of the present paper is to suggest that the same technique be used to determine directly the energy-*versus*-momentum curve for the excitations in liquid helium, and to predict some details of the experiment. A direct measurement of this curve would be of considerable interest, since the shape of the curve has already been predicted in some detail by indirect

methods. Landau² argued on theoretical grounds that the energy $E(k)$ of an excitation momentum $\hbar k$ should rise linearly with slope $\hbar c$ for small k (c = speed of sound = 240 m/sec), pass through a maximum, drop to a local minimum at some value k_0 , and rise again when $k > k_0$. For small k , the excitations are called phonons and may be thought of as quantized sound waves; the excitations with $k \sim k_0$ are called rotons, and seem to be the quantum-mechanical analog of smoke rings.^{3,4} At low temperatures, only the linear portion of the curve and the portion near the minimum are excited; if the curve is represented near the minimum by $E(k) = \Delta + \hbar^2(k - k_0)^2/2\mu$, the specific heat and second sound data can be fitted best with the values⁵

$$\Delta/\kappa = 9.6^\circ\text{K}, \quad k_0 = 2.30 \text{ \AA}^{-1}, \quad \mu = 0.40 m_{\text{He}},$$

and almost as well with the values²

$$\Delta/\kappa = 9.6^\circ\text{K}, \quad k_0 = 1.95 \text{ \AA}^{-1}, \quad \mu = 0.77 m_{\text{He}}.$$

A Landau-type curve has recently been obtained from first principles by the substitution of a trial function into a variational principle for the energy.^{3,4} The resulting curve is an upper limit to the true spectrum, and gives $\Delta/\kappa = 11.5^\circ\text{K}$, $k_0 = 1.85 \text{ \AA}^{-1}$, $\mu \sim 0.20$

* Richard C. Tolman Fellow.

¹ G. Placzek and L. Van Hove, *Phys. Rev.* **93**, 1207 (1954). We have recently learned that some of the ideas in the present paper have been discussed by V. V. Tolmachev, *Repts. Acad. Sci. U.S.S.R.* **101**, No. 6 (1955).

² L. Landau, *J. Phys. (U.S.S.R.)* **5**, 71 (1941); **11**, 91 (1947).

³ R. P. Feynman, *Phys. Rev.* **94**, 262 (1954).

⁴ R. P. Feynman and M. Cohen, *Phys. Rev.* **102**, 1189 (1956).

⁵ deKlerk, Hudson, and Pellam, *Phys. Rev.* **93**, 28 (1954).

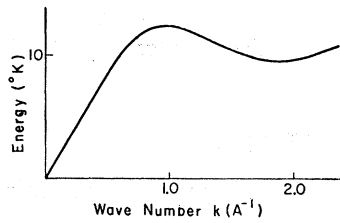


FIG. 1. A Landau-type energy-versus-momentum curve, with $\Delta = 9.6^\circ\text{K}$, $\mu = 1.06 m_{\text{He}}$, $k_0 = 1.85 \text{ \AA}^{-1}$.

m_{He} . In the rough computations of this paper we shall use the curve of Fig. 1, which has $\Delta/k = 9.6^\circ\text{K}$, $k_0 = 1.85 \text{ \AA}^{-1}$, $\mu = 1.06 m_{\text{He}}$. These values represent a compromise between theory and experiment, and also fit the specific heat data. Most of our numbers have only a qualitative significance, since the shape of the energy curve between the phonon and roton regions is highly uncertain.

II. GENERAL THEORY

Suppose the liquid is initially in state j , and we bombard it with neutrons of mass m and momentum $\hbar\mathbf{k}_i$; the cross section for a process in which the liquid is left in one of a group of final states F , and the neutron emerges with a momentum in some region G of \mathbf{k} space, is given by the Born approximation^{6,7} as

$$\sigma = \frac{2a^2}{k_i} \sum_{f \in F} \int_{\mathbf{k} \in G} |V_{fj}(\mathbf{k} - \mathbf{k}_i)|^2 \times \delta\left(k^2 - k_i^2 + \frac{2m}{\hbar^2}(E_f - E_j)\right) d\mathbf{k}, \quad (1)$$

where the sum and the integral extend over the regions F and G , respectively. The matrix elements V are given by

$$V_{fj}(\mathbf{q}) = \int \psi_f^*(\mathbf{r}_1, \dots, \mathbf{r}_N) \sum_{i=1}^N \times \exp(i\mathbf{q} \cdot \mathbf{r}_i) \psi_j(\mathbf{r}_1, \dots, \mathbf{r}_N) d\mathbf{r}_1 \dots d\mathbf{r}_N,$$

where ψ_j and ψ_f are the wave functions for the liquid in states j and f . The scattering length a is independent

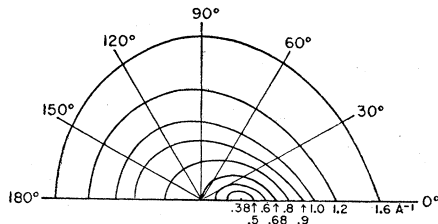


FIG. 2. Kinematics of production of single excitations. The curves give the wave number k_f of the exit neutron, as a function of k_i and θ ; k_i is the distance from the origin. On each curve k_i is constant and has the value given on the $\theta = 0$ axis. Note that $k_f = k_i$ when $\theta = 0$ (and $k_i > 0.68 \text{ \AA}^{-1}$).

⁶ G. Placzek, Phys. Rev. **86**, 377 (1952).

⁷ For the justification of the use of the Born approximation in this problem see E. Fermi, Ricerca sci. **7**, 13 (1936); G. Breit, Phys. Rev. **71**, 215 (1947).

of energy at low energies, and is related to the total cross section σ' of a bound He nucleus by $\sigma' = 4\pi a^2$. McReynolds⁸ found $\sigma' = 1.1 \pm 0.15$ barns.

In elastic scattering, the final state of the liquid is the same as the initial state.⁹ In the matrix element for elastic scattering, the integral of ψ_j^2 over all coordinates but one is equal to $1/V$ (V = volume of the liquid) except at points very close to the surface. Only the region near the surface contributes to the volume integral of $\exp(i\mathbf{q} \cdot \mathbf{r})$, and hence the only elastic scattering from the liquid is diffraction from the surface.¹⁰ In a crystal, the integral of ψ_j^2 over all coordinates but one gives a function which is strongly peaked at the lattice points; hence for certain directions of \mathbf{q} the matrix element $V_{fj}(\mathbf{q})$ becomes proportional to N , and elastic scattering occurs. Therefore, although neutrons are scattered elastically from solids, virtually no elastic scattering should occur from the liquid.

III. SCATTERING AT ZERO TEMPERATURE

If the liquid is at zero temperature, then the initial state is the ground state ψ_0 , and the neutron must lose energy in the scattering. The simplest process which can occur is the creation of a single excitation of momentum $\hbar(\mathbf{k}_i - \mathbf{k}_f)$ in the liquid (if we impose periodic boundary conditions on the liquid, the stationary states may be taken as momentum eigenstates). Energy conservation requires

$$\hbar^2 k_i^2 / 2m = \hbar^2 k_f^2 / 2m + E(|\mathbf{k}_i - \mathbf{k}_f|). \quad (2)$$

If we fix \mathbf{k}_i and the angle θ between \mathbf{k}_i and \mathbf{k}_f , then if $k_i > 0.68 \text{ \AA}^{-1}$ ($\lambda_i < 9.25 \text{ \AA}$) there is a unique k_f for each θ . When k_i is just less than 0.68 \AA^{-1} , (2) becomes insoluble for $\theta > 90^\circ$. As k_i decreases further, the region of solubility of (2) is a cone of decreasing aperture about the forward direction. For each direction θ in the cone there are two solutions for k_f . Finally, when $k_i < 0.38 \text{ \AA}^{-1}$, (2) becomes insoluble at any angle. The qualitative behavior of the solutions of (2) is shown in Fig. 2, but not too much significance should be attached to the numbers, which are based on the uncertain curve of Fig. 1.

The solutions of (2) should appear as lines in the

⁸ A. W. McReynolds, Phys. Rev. **84**, 969 (1951).

⁹ This is true if the liquid is confined in a fixed box. If the box is free to recoil, then for elastic scattering the final state is the same as the initial state except for a translational motion of the whole with momentum $\hbar(\mathbf{k}_i - \mathbf{k}_f)$ and infinitesimal energy $\hbar^2(\mathbf{k}_i - \mathbf{k}_f)^2 / 2Nm_{\text{He}}$. The wave function for the final state is then $\psi_f = \psi_i \exp[iN^{-1}(\mathbf{k}_i - \mathbf{k}_f) \cdot \sum \mathbf{r}_i]$. The remaining arguments are still valid, with each \mathbf{r}_i being measured from the center of mass rather than from an origin determined by the location of the box.

¹⁰ By "elastic scattering" we mean scattering processes in which the incident and exit neutrons have the same energy, and furthermore the state of the liquid is unchanged. If we relax the latter requirement, then at finite temperature some neutrons can scatter without energy loss by colliding with excitations in the liquid. However, neutrons which are scattered by collisions with excitations emerge with a continuous distribution of energies (i.e., the number in any energy range dE is proportional to dE), and there will not be any "group" of elastically scattered neutrons.

energy spectrum of the neutrons emerging at a given angle. The energy-*versus*-momentum curve for the excitations can be obtained from Eq. (2) by measuring k_f as a function of angle for fixed k_i , or by looking at a fixed exit angle and varying k_i . Processes involving multiple excitations contribute a continuous background. When $k_i < 0.38 \text{ \AA}^{-1}$, the right side of (2) is bigger than the left for any k_f ; furthermore, since $E(k)$ is the energy of the lowest state of the liquid having momentum $\hbar\mathbf{k}$, production of multiple excitations will also be impossible when $k_i < 0.38 \text{ \AA}^{-1}$. Hence, when the liquid is at zero temperature, neutrons with $k_i < 0.38 \text{ \AA}^{-1}$ ($\lambda > 16.5 \text{ \AA}$) should pass through with no scattering. This conclusion seems consistent with the data of Sommers, Dash, and Goldstein¹¹ on the transmission of neutrons by He.

The strengths of the lines are given by (1). We take the region G of k space as $k^2 \Delta k d\Omega$, where Δk includes the line under study. Momentum conservation manifests itself in the vanishing of $V_{f0}(\mathbf{k}-\mathbf{k}_i)$ unless the state f has the momentum $\hbar(\mathbf{k}_i-\mathbf{k})$. Integration of (1) over G gives

$$\frac{d\sigma_1}{d\Omega} = a^2 \frac{k_f}{k_i} \frac{|V_{f0}(\mathbf{k}_f-\mathbf{k}_i)|^2 d\Omega}{\left| 1 + \frac{m E'(|\mathbf{k}_f-\mathbf{k}_i|)}{\hbar^2 |\mathbf{k}_f-\mathbf{k}_i|} \left(1 - \frac{k_i}{k_f} \cos\theta \right) \right|^2} \quad (3)$$

as the cross section for scattering into $d\Omega$ with the production of one excitation of momentum $\hbar(\mathbf{k}_i-\mathbf{k}_f)$ (and final neutron momentum $\hbar\mathbf{k}_f$). In reference 3 the function

$$\psi_k = \mathcal{G}^{-1/2} \psi_0 \sum \exp(i\mathbf{k} \cdot \mathbf{r}_i) \quad (4)$$

is proposed to represent a single excitation of momentum $\hbar\mathbf{k}$. This function is exact for very small k , and gives an energy spectrum qualitatively similar to Landau's, but with Δ twice too large. Normalization requires $\mathcal{G} = NS(k)$, where $S(k)$ is the Fourier transform of the zero-temperature radial distribution function $p(r)$,

$$S(k) = \int \exp(i\mathbf{k} \cdot \mathbf{r}) p(r) d\mathbf{r}.$$

The resulting matrix element is

$$|V_{f0}(\mathbf{q})|^2 = NS(q). \quad (5)$$

Actually, (5) is an over-estimate, as one can see from the exact sum rule

$$\sum_f |V_{f0}(\mathbf{q})|^2 = [V(\mathbf{q})V^*(\mathbf{q})]_{00} = NS(q). \quad (6)$$

If (5) were exact, then (6) would imply that production of multiple excitations is impossible. A more accurate wave function for an excitation is given in reference 4, and leads to the matrix elements given in Fig. 3. In the roton region, these matrix elements are only ten to fifteen percent smaller than those given by (5), and

¹¹ Sommers, Dash, and Goldstein, Phys. Rev. **97**, 855 (1955).

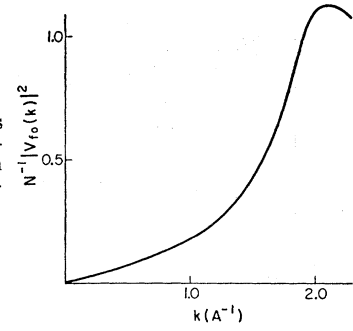


FIG. 3. Matrix elements for production of single excitations, computed from the wave functions of reference 4.

we infer that the most likely way for a neutron to lose a given amount of momentum is through the production of a single excitation.

Substituting the matrix elements of Fig. 3 into Eq. (3), we obtain the curves of Fig. 4, giving the angular variation of line strength for different values of k_i . The curves are given in units of a^2 , which is the differential cross section per unit solid angle for scattering from a bound helium nucleus. When $k_i > 0.68 \text{ \AA}^{-1}$, $d\sigma_1/d\Omega$ vanishes at $\theta=0$ because the matrix element V_{f0} approaches zero when the momentum transfer is small. When $k_i < 0.68 \text{ \AA}^{-1}$, there are two curves for each k_i , corresponding to the two lines which are observed at each angle within the cone of solubility of (2). At the edges of this cone, $d\sigma_1/d\Omega$ becomes infinite because the denominator of (3) vanishes. The total cross section, however, is finite.

If we neglect the possibility of producing multiple excitations, the total cross section at zero temperature is obtained by integrating (3) over angles. The resulting cross sections are compared in Fig. 5 with the total cross sections measured¹¹ at 1.25°K (the temperature effect, which is negligible, is discussed in the next section). The agreement of theory and experiment within 30% is quite satisfactory in view of our incomplete knowledge of the wave function ψ_f and the curve $E(k)$. When k_i is large, Eq. (1) can be shown to lead to the total cross section $(16/25)4\pi a^2 N$, which is just the cross section for free helium nuclei scattering incoherently. The theoretical curve has been extra-

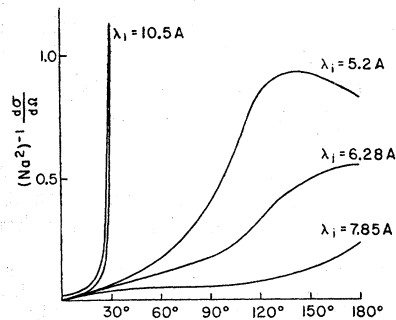


FIG. 4. Angular distribution of neutrons which have been scattered by the process of producing a single excitation, at zero temperature.

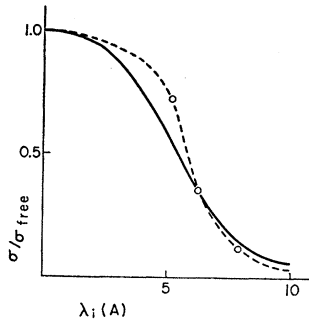


FIG. 5. The broken line is the total cross section computed here. Circles are computed points. The solid line represents the measurements of Sommers *et al.* at 1.25°K.

polated to this value. As λ decreases, the theoretical curve rises faster than the experimental one; the reason is probably that the matrix elements of Fig. 3 are too large when the momentum transfer is in the roton region. To see this more clearly, we note that there is an exact sum rule,

$$\sum_f |V_{of}(\mathbf{k})|^2 (E_f - E_0) = [V^*(\mathbf{k})(H - E_0)V(\mathbf{k})]_{00} = N\hbar^2 k^2 / 2m, \quad (7)$$

which, in conjunction with Eq. (6), says that the “average” energy loss associated with momentum transfer $\hbar\mathbf{k}$ is $\hbar^2 k^2 / 2mS(k)$. For small k , this “average” energy loss is the same as $E(k)$; hence the idea that multiple excitations are produced with negligible probability is correct. However, when $k = 1.85 \text{ \AA}^{-1}$, one finds that the “average” energy loss is 19.5°K, which is twice the size of $E(k)$. If the matrix elements of Fig. 3 are correct, then the sum rule (6) implies that there is only a 13% probability of producing multiple excitations when the momentum transfer is 1.85 \AA^{-1} . Such a small probability of multiple excitation seems hardly consistent with a mean energy loss corresponding to the production of two rotons. We conclude that the correct matrix elements for single roton production are almost certainly smaller than those given in Fig. 3.¹²

IV. EFFECTS OF FINITE TEMPERATURE

If the liquid is at a finite temperature, some phonons and rotons are always present, and the neutrons can gain energy by annihilating excitations. The energy spectrum of the neutrons emerging at a given angle will contain a line representing annihilation of single excitations as well as a line or lines arising from their production. At temperatures below the λ point, the production process is far more important than annihilation if the wavelength of the incident neutrons is less than 10 Å. Since phonons and rotons obey Bose statistics, the rate of annihilation of excitations of momentum $\hbar\mathbf{k}$ is proportional to the number $n(\mathbf{k})$ of

¹² It is not entirely obvious that the total cross section is lowered by lowering the probability of producing single excitations, since the sum rule (6) implies that the probability of producing multiple excitations must be correspondingly increased. However, the density-of-states factor resulting from the delta function in Eq. (1) produces a decrease in the total cross section when probability is transferred from single to multiple excitations.

such excitations already present, while the rate of production is proportional to $n(\mathbf{k}) + 1$. At temperature T , we have $n(\mathbf{k}) = \{\exp[E(\mathbf{k})/\kappa T] - 1\}^{-1}$; for rotons at 2°, $E(k)/\kappa T \approx 5$, and we see that the “spontaneous production” factor 1 is much greater than $n(\mathbf{k})$. Figure 2 shows that if the incident neutron wavelength is less than 10 Å ($k_i \gtrsim 0.6 \text{ \AA}^{-1}$), most of the excitations produced have wave numbers greater than 0.4 \AA^{-1} and consequently energies large compared to 2°K. Furthermore, Fig. 3 shows that the matrix elements for the production of low-energy phonons are small. Thus we see that in the range $T \lesssim 2^\circ\text{K}$, $\lambda \lesssim 10 \text{ \AA}$, spontaneous production is much more important than “induced production” and annihilation, and the lack of temperature dependence of the total cross section is understood.

For incident neutrons of wavelength greater than $\sim 10 \text{ \AA}$, it is kinematically impossible to produce any except very low-energy phonons (and no excitations at all can be produced when $\lambda > 16.5 \text{ \AA}$). Hence the annihilation process is the most important one at long neutron wavelengths, and the total cross section in this region is strongly temperature-dependent. Ultimately, at very long incident neutron wavelengths, the kinematics becomes that of zero-energy incident neutrons. Figure 2 shows that a zero-energy incident neutron can annihilate only phonons with wave number $k = 0.68 \text{ \AA}^{-1}$ and energy 11°K.¹³ The total cross section ultimately depends on the temperature as $\exp(-11/T)$, and on the incident velocity as $1/v$ [arising from the factor $1/k_i$ in Eq. (1)].

V. RESOLUTION AND LINE WIDTH

In order to obtain even a moderately accurate measurement of the roton energy Δ , the velocities of the incident and exit neutrons must be known very accurately. Figure 2 shows that the slowest neutron which can produce a minimum energy roton has a wave number $k \sim 1.04 \text{ \AA}^{-1}$ (energy = 25°); the exit neutron in this case has $k \sim 0.81 \text{ \AA}^{-1}$ (energy = 15°). To measure Δ with an accuracy of one degree, the neutron energies must be accurate to 0.7°; for the incident neutrons, we need $\delta\lambda/\lambda = \delta E/2E = 0.7/50 = 0.014$. Thus, to measure Δ with ten percent accuracy, the velocity spread of the incident neutron beam must be limited to about one percent. Nothing is gained by studying neutrons which have annihilated a roton; the slowest incident neutron which can annihilate a roton has $k \sim 0.81 \text{ \AA}^{-1}$, and we need $\delta\lambda/\lambda = 0.7/30 = 0.023$. The slight improvement in the resolution situation is far more than offset by the low rate of annihilation, as compared with production (see Sec. IV). The resolution situation is best when we observe neutrons scattered through 180°. If we study

¹³ This is not entirely correct, since annihilation of multiple excitations is possible, though unlikely at low temperatures. The total momentum of the excitations annihilated must be at least 0.68 \AA^{-1} and the total energy at least 11°K. At low temperatures and velocities, the cross section still varies as $v^{-1} \exp(-11/T)$.

the 90° scattering, the slowest allowed incident neutron has $k \sim 1.5 \text{ \AA}^{-1}$ and we need $\delta\lambda/\lambda \sim 0.007$.

If one looks at the energy distribution of the neutrons emerging at a particular angle, how broad is the line corresponding to those neutrons which have created a roton? We have studied this question in some detail; in the Appendix we compute the detailed line shape which would result if we make certain assumptions about the interaction between phonons and rotons. The assumptions prove to be unrealistic, but the method of computation is of some interest. The result which we obtain for the line width is what one would expect from the uncertainty principle; the width is \hbar/τ , where τ is the lifetime of the roton until it collides with something. In our model, roton-roton interactions are neglected; hence the lifetime we compute is that for roton-phonon collisions. This lifetime is very long, and the resulting width is less than 10^{-6} K (to be compared with a roton energy $\Delta = 9.6 \text{ K}$) when the helium is at a temperature of 1° K . Landau and Khalatnikov¹⁴ have computed the lifetimes for phonon-phonon, phonon-roton, and roton-roton collisions. They find that at temperatures of 1° and higher, the roton-roton lifetime is much shorter than the roton-phonon lifetime. When $T = 1^\circ$, the width of a roton line is 0.006 K , which is still very small compared with the roton energy, but large compared with 10^{-6} K . The width is proportional to $T^{3/2} \exp(-\Delta/kT)$, which represents the temperature dependence of the number of rotons present; when $T = 2^\circ \text{ K}$, the width is about 1° . Similarly, one can compute the width of a line arising from the production of phonons by neutrons; when $T = 1^\circ \text{ K}$, the lifetimes of a phonon for scattering by a roton or by another phonon are comparable, both giving rise to widths of about 10^{-5} K . We conclude that for all practical purposes the lines in the neutron spectrum will be true delta functions if the helium temperature is near 1° K .

To calculate the cross section for roton-roton collisions, Landau and Khalatnikov assume a delta-function interaction between rotons, the strength of the interaction being chosen to fit viscosity data. In the appendix we show that such a delta-function potential, with a strength close to that of Landau and Khalatnikov, arises from the possibility that roton I can emit a phonon which is subsequently absorbed by roton II. The result is only suggestive rather than conclusive, however, since we are also led to a velocity-dependent interaction between rotons, comparable in strength with the delta function.

ACKNOWLEDGMENTS

We wish to thank P. J. Bendt, M. Gell-Mann, W. J. Karzas, and H. Palevsky for valuable discussions.

¹⁴ L. Landau and I. M. Khalatnikov, J. Exptl. Theoret. Phys. U.S.S.R. **19**, 637, 709 (1949).

APPENDIX

The problem of the breadth and shape of the lines in the neutron spectrum caused us some confusion, the details of which are not worth recounting. Finally, we constructed a "model" Hamiltonian for helium, including a phonon-roton interaction, for which the line shape can be computed very accurately. Analysis of this Hamiltonian not only resolved our private confusion, but also showed what the line shape is in the case of real helium. The important features of the answer can be obtained from perturbation theory, provided certain linear terms are interpreted as the beginning of exponentials. We regard the more accurate computation as sufficiently interesting to be presented here. It is analogous to the Weisskopf-Wigner method in the theory of optical spectra.

Suppose, for simplicity, that excitations with $k < k_c$ are phonons, with energy $E(k) = \hbar ck$, and excitations with $k > k_c$ are rotons with energy $E(k) = \Delta + \hbar^2(k - k_0)^2/2\mu$. If there were no interaction between phonons and rotons, the Hamiltonian for the liquid would be $H = \sum a_k^* a_k E(k)$, where a_k^* and a_k are the usual creation and destruction operators for excitations of momentum $\hbar k$; the operator $a_k^* a_k$ has integral eigenvalues n_k , which represent the number of excitations present with momentum $\hbar k$. The matter density at \mathbf{r} is given by

$$\rho(\mathbf{r}) - \rho_0 = (\rho_0 \hbar / 2Vc)^{1/2} \sum_{k < k_c} k^{1/2} \times [a_k \exp(i\mathbf{k} \cdot \mathbf{r}) + a_k^* \exp(-i\mathbf{k} \cdot \mathbf{r})].$$

We are interested only in the average behavior of the matter density over a region of finite size (the size of the roton) and have therefore omitted wavelengths smaller than $2\pi/k_c$ in the representation of $\rho(\mathbf{r})$. We assume that if a roton of momentum $\hbar \mathbf{k}_i$ is at \mathbf{r} , its energy is $E(k) + (\partial\Delta/\partial\rho)[\rho(\mathbf{r}) - \rho_0]$. Atkins and Edwards¹⁵ have measured $\partial\Delta/\partial\rho$ and find $\partial\Delta/\partial\rho = -0.57\Delta/\rho$. The actual interaction between phonons and rotons involves further coupling terms, which will be discussed later.

It is convenient to use a mixed representation in which phonons are treated with creation and destruction operators, and rotons are represented as particles with coordinates and momenta. If the number of rotons present is m , the Hamiltonian is

$$H = \sum_{k < k_c} a_k^* a_k \hbar ck + \sum_{i=1}^m E(\mathbf{k}_i) + \frac{\partial\Delta}{\partial\rho} (\rho_0 \hbar / 2Vc)^{1/2} \sum_{i=1}^m \times \sum_{k < k_c} k^{1/2} [a_k \exp(i\mathbf{k} \cdot \mathbf{r}_i) + a_k^* \exp(-i\mathbf{k} \cdot \mathbf{r}_i)]. \quad (1')$$

The interaction term in (1') creates and destroys single phonons, since the operators a_k and a_k^* appear linearly.

¹⁵ K. R. Atkins and M. H. Edwards, Phys. Rev. **97**, 1429 (1955).



FIG. 6. Diagrams representing the phonon-rotor interaction in the Hamiltonian (1'). The solid line is a roton, the broken line a phonon. Time increases from left to right. Diagram (a) represents emission of a phonon, and (b) represents absorption.

Rotons only change their momenta, however, since the interaction merely multiplies the roton wave function by a plane wave. If we represent rotors by solid lines and phonons by dotted lines, the two terms in the phonon-rotor interaction can be represented by the diagrams of Fig. 6.

If the number of neutrons per second emerging in solid angle $d\Omega$ with an energy loss in the range $(E, E+dE)$ is $n(E)dEd\Omega$, the Fourier transform of $n(E)$ is given by Eq. (1) as

$$f(\eta) = \int_{-\infty}^{\infty} \exp(-i\eta E) n(E) dE \\ = \left(\frac{2a^2\hbar}{m} \right) \int k^2 dk \sum_j \exp[-i\eta(E_f - E_j)] \\ \times |V_{fj}(\mathbf{k} - \mathbf{k}_i)|^2 \delta\left(k^2 - k_j^2 + \frac{2m}{\hbar^2}(E_f - E_j)\right).$$

Since the energy needed to produce a roton is small compared with the energy of the incident neutrons, the term $(E_f - E_j)$ in the argument of the delta function can be ignored with negligible error. This approximation gets better as the incident neutrons get faster.¹⁶ Similarly, since the direction of \mathbf{k} is fixed and its length is very close to k_i , we can replace $\mathbf{k} - \mathbf{k}_i$ by a constant vector \mathbf{q} , where $|\mathbf{q}| = 2k_i \sin(\theta/2)$. Furthermore, the liquid may be in different initial states j with probability $\exp(-\beta E_j) / \sum \exp(-\beta E_j)$, where $\beta = 1/kT$. Thus we obtain

$$f(\eta) = (a^2\hbar k_i/m) \left[\sum_{i,j} \exp(-\beta E_j) \right]^{-1} \sum_{i,j} \\ \times \exp\{-[\beta E_j + i\eta(E_f - E_j)]\} |V_{fj}(q)|^2 \\ = (a^2\hbar k_i/m) [\text{Tr} \exp(-\beta H)]^{-1} \\ \times \text{Tr}[V \exp(-i\eta H) V^* \exp(-\beta H + i\eta H)]. \quad (2')$$

In Eq. (4) we have suggested that the wave function for a single roton of momentum \mathbf{q} is the ground-state wave function multiplied by $\sum \exp(i\mathbf{q} \cdot \mathbf{r}_i)$. Since the wave function for an oscillator in its first excited state is just the ground-state wave function multiplied by the normal coordinate of the oscillator, it would follow that $\sum \exp(i\mathbf{q} \cdot \mathbf{r}_i)$ is the normal coordinate for rotors of momentum \mathbf{q} . In particular, if $|j\rangle$ is a state contain-

¹⁶ We are only computing the shape of $n(E)$ for energies near the roton energy. Fast neutrons tend also to produce multiple excitations, with large energy losses, but we are not studying that part of the spectrum.

ing no rotors of momentum \mathbf{q} , then

$$V|j\rangle = \sum \exp(i\mathbf{q} \cdot \mathbf{r}_i) |j\rangle \\ = [NS(q)/V]^{\frac{1}{2}} \exp(i\mathbf{q} \cdot \mathbf{r}) |j\rangle. \quad (3')$$

The wave function $\exp(i\mathbf{q} \cdot \mathbf{r}) |j\rangle$ represents whatever was present in the initial state j , plus a roton of momentum \mathbf{q} ; \mathbf{r} is the position coordinate of the roton. If $|j\rangle$ already contains rotors of momentum q , then $\sum \exp(i\mathbf{q} \cdot \mathbf{r}_i)$ both creates and destroys rotors. Actually, $\sum \exp(i\mathbf{q} \cdot \mathbf{r}_i)$ is not the exact normal coordinate for a roton, and consequently this factor can also create and destroy multiple excitations. In keeping with the spirit of this computation, we deal with a fictitious model in which direct production of multiple excitations by neutrons does not occur. This does not mean that no multiple excitations are produced; a neutron can produce a single virtual roton, which then breaks up into a real roton and a real phonon through the interaction term in H .

As a further simplification, we deal with a case slightly different from thermodynamic equilibrium. In the initial states j we allow an arbitrary number of phonons to be present, with the usual thermodynamic distribution; however, we consider only initial states in which no rotors are present. This picture is accurate at low temperatures. Consequently, for the initial states j the Hamiltonian is

$$H_0 = \sum_{k < k_c} a_k^* a_k \hbar c k, \quad (4')$$

and for the final states f

$$H = H_0 + E(\mathbf{k}) + \partial\Delta/\partial\rho (\rho_0\hbar/2Vc)^{\frac{1}{2}} \sum_{k < k_c} k^{\frac{1}{2}} \\ \times [a_k \exp(ik \cdot \mathbf{r}) + a_k^* \exp(-ik \cdot \mathbf{r})] \quad (5') \\ = H_0 + H_1.$$

In determining the traces of (2') we can use any states as a basis. For the initial states we use eigenstates of H_0 , denoted by $|n_{k_1} n_{k_2} \dots\rangle$; as base vectors for the states with a roton present we use products of an eigenstate of H_0 and a position eigenfunction (delta function) for the roton, denoted by $|\mathbf{x}; n_{k_1} n_{k_2} \dots\rangle$. Since we deal only with initial states with no rotors,

$$[\text{Tr} \exp(-\beta H)]^{-1} = \prod_{k < k_c} [1 - \exp(-\beta \hbar c k)].$$

For the other trace we obtain

$$\text{Tr}[V \exp(-i\eta H) V^* \exp(-\beta H + i\eta H)] \\ = \sum_{n_{k_1}, n_{k_2}, \dots} \int dx dy \langle n_{k_1} n_{k_2} \dots | V | \mathbf{y}; n_{k_1} n_{k_2} \dots \rangle \\ \times \langle \mathbf{y}; n_{k_1} n_{k_2} \dots | \exp[-i\eta(H_0 + H_1)] | \mathbf{x}; n_{k_1} n_{k_2} \dots \rangle \\ \times \langle \mathbf{x}; n_{k_1} n_{k_2} \dots | V^* | n_{k_1} n_{k_2} \dots \rangle \\ \times \exp[(-\beta + i\eta) \sum_{k < k_c} n_k \hbar c k]. \quad (6')$$

From (3') it follows that

$$\begin{aligned} \langle n_{\mathbf{k}_1} n_{\mathbf{k}_2} \cdots | V | \mathbf{y}; n_{\mathbf{k}_1} n_{\mathbf{k}_2} \cdots \rangle &= [NS(q)/V]^{\frac{1}{2}} \exp(i\mathbf{q} \cdot \mathbf{y}), \\ \langle \mathbf{x}; n_{\mathbf{k}_1} n_{\mathbf{k}_2} \cdots | V^* | n_{\mathbf{k}_1} n_{\mathbf{k}_2} \cdots \rangle &= [NS(q)/V]^{\frac{1}{2}} \exp(-i\mathbf{q} \cdot \mathbf{x}). \end{aligned}$$

A great simplification is effected if we neglect the dependence of $E(\mathbf{k})$ on \mathbf{k} , i.e., let $E(\mathbf{k}) = \Delta$. We now make this approximation and shall later consider the effects of restoring the dependence. Since H does not involve the momentum of the roton, if the wave function is initially a position eigenfunction of the roton it will remain a position eigenfunction. Consequently,

$$\begin{aligned} \langle \mathbf{y}; n_{\mathbf{k}_1} n_{\mathbf{k}_2} \cdots | \exp[-i\eta(H_0 + H_1)] | \mathbf{x}; n_{\mathbf{k}_1} n_{\mathbf{k}_2} \cdots \rangle \\ = \delta(\mathbf{x} - \mathbf{y}) \langle \mathbf{x}; n_{\mathbf{k}_1} n_{\mathbf{k}_2} \cdots | \\ \exp[-i\eta(H_0 + H_1)] | \mathbf{x}; n_{\mathbf{k}_1} n_{\mathbf{k}_2} \cdots \rangle. \end{aligned} \quad (7')$$

The second factor on the right is simply a diagonal element of the Green's function (represented in occupation-number space) for a collection of oscillators forced by the function H_1 . The matrix elements G_{mn} for a forced oscillator are easily worked out, by operator calculus¹⁷ or other methods. If the Hamiltonian for a forced oscillator is

$$H = a^* a \epsilon + g(t) a + g^*(t) a^*, \quad (8')$$

and $|m\rangle$ and $|n\rangle$ are eigenstates of the unforced oscillator with energies $m\epsilon$ and $n\epsilon$, respectively, then

$$\begin{aligned} G_{mn} &= \langle m | \exp\left[-i \int_{t'}^{t''} H(t) dt\right] | n \rangle \\ &= \exp(i\epsilon m t' - i\epsilon n t'') (m! n!)^{-\frac{1}{2}} \sum_r \binom{m}{r} \binom{n}{r} r! \\ &\quad \times (-iB^*)^{m-r} (-iB)^{n-r} G_{00}, \end{aligned} \quad (9')$$

where

$$B = \int_{t'}^{t''} g(t) \exp(-i\epsilon t) dt,$$

and

$$G_{00} = \exp\left(- \int_{t'' > t > t'} dt ds g(t) g^*(s) e^{-i\epsilon(t-s)}\right).$$

The trace is now easily obtained. We find

$$\begin{aligned} \sum_n \exp[(-\beta + i t'' - i t') \epsilon n] G_{nn} \\ = G_{00} \sum_{n \geq r \geq 0} \frac{e^{-\beta \epsilon n} n!}{r! [(n-r)!]^2} (-BB^*)^{n-r} \\ = G_{00} (1 - e^{-\beta \epsilon})^{-1} \exp[-BB^*/(e^{\beta \epsilon} - 1)]. \end{aligned} \quad (10')$$

From (5') we have $g(t) = (\partial \Delta / \partial \rho) (\rho_0 \hbar / 2V_c)^{\frac{1}{2}} k^{\frac{1}{2}} e^{i\mathbf{k} \cdot \mathbf{r}}$. Replacing the sum over oscillators by $V(2\pi)^{-3} \int d\mathbf{k}$,

¹⁷ See, for instance, R. P. Feynman, Phys. Rev. **84**, 108 (1951), Eq. (38). The present case is a trivial generalization of the result given there.

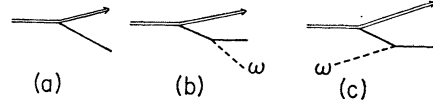


FIG. 7. Interaction of neutron (double line) with helium. In (a) the neutron produces a real roton. In (b) the neutron produces a virtual roton which decays into a real roton plus a phonon of frequency ω . In (c) the virtual roton absorbs a phonon and becomes a real roton.

we find [letting $\alpha = (\partial \Delta / \partial \rho) (\rho_0 \hbar / c)^{\frac{1}{2}}$]

$$\begin{aligned} f(\eta) &= (\alpha^2 \hbar k_i / m) NS(q) \exp(-i\Delta \eta) \\ &\quad \times \exp\left\{ -\frac{\alpha^2}{(2\pi)^2 (\hbar c)^4} \int_0^{\hbar c k_e} d\omega \left[-i\eta \omega^2 \right. \right. \\ &\quad \left. \left. - \omega (e^{-i\omega \eta} - 1) + \frac{4\omega \sin^2(\omega \eta / 2)}{e^{\beta \omega} - 1} \right] \right\}. \end{aligned} \quad (11')$$

The various terms in the exponent of (11') are easily understood by applying perturbation theory to (5'), treating α as small. The coefficient of $-i\eta$ is simply the energy Δ of a roton, plus a correction arising from the fact that the roton can emit and reabsorb, or absorb and re-emit, phonons. The rate of emission and reabsorption of phonons of momentum $\hbar \mathbf{k}$ is proportional to $n_{\mathbf{k}} + 1$, while the rate of absorption and re-emission is proportional to $n_{\mathbf{k}}$, with an energy denominator of equal magnitude but opposite sign. Hence, the energy correction is independent of the number of phonons present, and does not depend on the temperature. The numerical value of the self-energy is $\delta E / \Delta = -0.04 k_e^3$, with k_e measured in reciprocal angstroms. The cutoff k_e should correspond to a wavelength equal to the roton size, i.e., several interatomic spacings; we estimate $k_e \sim 0.5 \text{ \AA}^{-1}$.

The remaining terms in the exponent represent the possibility of production of multiple excitations [Fig. 7(b)], or production of a roton which then absorbs a phonon [Fig. 7(c)]. In all diagrams the neutron (double line) interacts with the liquid only once, and produces a roton. The roton may then emit or absorb an arbitrary number of phonons, each roton-phonon interaction contributing a factor α to the amplitude and α^2 to the probability. The only processes with rates proportional to α^2 are those shown in Figs. 7(b) and 7(c). In 7(b) the neutron suffers an energy loss $\Delta + \omega$, while in 7(c) the energy loss is $\Delta - \omega$. The rate of 7(b) is proportional to $n(\omega) + 1$, while 7(c) is proportional to $n(\omega)$. Hence at low temperatures the line shape is strongly asymmetric. If the exponent of (11') is expanded into complex exponentials, the coefficient of $\exp(-i\omega \eta)$ is the rate of 7(b) as computed in perturbation theory, and the coefficient of $\exp(i\omega \eta)$ is the rate of 7(c). The remaining term, which is independent of η , represents a change in the rate of single roton production 7(a) arising from the

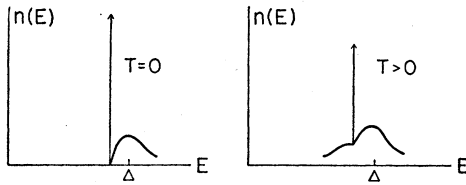


FIG. 8. Shape of a line in the neutron spectrum resulting from roton production, computed from (11'). In the actual case, the delta-functions (represented by arrows) are slightly smeared out, but the rest of the shape is as shown.

distortion of the single-roton wave function by virtual phonons.

Since α is small, the exponential in (11') can be accurately replaced by the first two terms of a power series. Then $n(E)$ is just the coefficient of $\exp(-iE\eta)$, and we can plot the line form (Fig. 8). If only the first two terms of the power series were retained, $n(E)$ would cut off sharply at energies more than $\hbar ck_c$ from the line center; the higher terms in the power series smear out the cutoff. The one-sidedness of the curve for $T=0$ arises from the fact that the roton is the lowest excitation of momentum \mathbf{q} . Since no annihilation is possible at zero temperature, the neutron cannot lose any less energy than that needed to produce a roton.

At high temperatures ($\beta\hbar ck_c \ll 1$) the line becomes Gaussian with width

$$\sigma^2 = \langle (E - \bar{E})^2 \rangle_{av} = \frac{1}{6\pi^2} \left(\frac{\partial \Delta}{\partial \rho} \right)^2 \frac{\rho_0 k_c^3}{\beta c^2}. \quad (12')$$

It is readily shown that in thermal equilibrium the matter density fluctuates according to the Gaussian distribution. The width of the Gaussian at high temperatures is $\rho_0 k_c^3 / 6\pi^2 \beta c^2$. Reasoning classically, one might say that although we do not know the value of the density at the place where the roton is created, nevertheless the density has an instantaneous value, which determines the amount of energy needed to create the roton. Accordingly, the line shape would be the same as the shape of the statistical distribution of the density fluctuations, as is indeed the case at high temperatures.

The classical argument fails at low temperatures, especially near the line center. For large values of η , $\sin^2(\omega\eta/2)$ may be replaced by its average value. The integral $\int d\omega \omega \exp(-i\omega\eta)$ approaches zero because of the oscillation of the exponential, and we find that $f(\eta) \sim \text{const} \times \exp[-i(\Delta + \delta E)\eta]$. Therefore $n(E)$ contains a delta function at the center of the line (the strength of the delta function approaches zero for large T). To understand this classically, we would have to say that there is a finite chance that the density is exactly equal to ρ_0 at the place where the roton is created; this, of course, is wrong. Since the density operator does not commute with the Hamiltonian, a density measurement would change the state of the system. Consequently, as in the double-slit experiment,

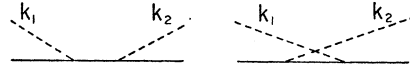


FIG. 9. Diagrams representing phonon-roton scattering.

the different possible outcomes can interfere with each other. Amplitudes, rather than probabilities must be added. Part of our uncertainty about the density comes from the fact that we do not know what state the liquid is in, because the temperature is finite; and part of the uncertainty is the quantum-mechanical uncertainty which still exists when the system is in a pure state. The former is correctly analyzable by classical reasoning, and the latter is not. Accordingly, one might say that a finite fraction of the density fluctuations is congenitally unobservable; this fraction gives rise to the delta function.

The uncertainty principle says that the width of a line arising from roton production is inversely proportional to the lifetime of the roton. Since there is nothing in the Hamiltonian (5') which would allow the roton to disintegrate,¹⁸ the "lifetime" is the time till the roton is scattered by a phonon. The two diagrams of Fig. 9 contribute to the scattering. If all rotons have the same energy, then energy conservation requires $k_1 = k_2$. Then the energy denominators for the two diagrams are equal in magnitude and opposite in sign, and the scattering rate is zero. This result also holds true in higher orders and is well known in meson theory. Hence the lifetime of the roton is infinite, and the line width zero.

We expect the delta function to spread out if we can analyze the Hamiltonian (5'), including the momentum dependence of $E(k)$. The width, presumably, will be the rate of scattering of rotons by phonons.¹⁹ We thought it worthwhile to extend our analysis to include this case, since it is not entirely obvious that the roton has a finite lifetime, in the sense required by the uncertainty principle, simply because it can scatter. Furthermore, the occurrence of delta functions is not clearly precluded by the uncertainty principle; a line form consisting of a delta function super-imposed on the center of (say) a Gaussian would have a finite energy spread. Therefore we continue the analysis.

The Lagrangian form of quantum mechanics²⁰ is useful here. In reference 20 the problem of a particle interacting with an oscillator has been studied. Suppose the total Hamiltonian is

$$H = H_{\text{part}} + a^* a \epsilon + g(x, t) a + g^*(x, t) a^* = H_{\text{part}} + H',$$

¹⁸ A roton cannot emit a real phonon, since the roton is the lowest state of given momentum.

¹⁹ Another way to see that the delta function must spread out is to note that $n(\mathbf{q}, E)$ is the Fourier transform in space and time of the "time-dependent pair distribution function" $p(\mathbf{r}, t)$, which is the probability of finding an atom at \mathbf{r} at time t , if there was an atom at the origin at $t=0$ [see L. Van Hove, Phys. Rev. **95**, 249 (1954)]. If $n(\mathbf{q}, E)$ contained a delta function for some E , it would follow that $\int p(\mathbf{r}, t) \exp(i\mathbf{q} \cdot \mathbf{r}) d\mathbf{r}$ does not approach zero for large t . But $p(\mathbf{r}, t)$ clearly becomes independent of \mathbf{r} and t for large t , and the integral must approach zero.

²⁰ R. P. Feynman, Revs. Modern Phys. **20**, 367 (1948).

where \mathbf{x} is the particle coordinate, and H_{part} is derivable from a Lagrangian L . Then the amplitude for the oscillator to go from state n at time t' to state m at time t'' , while the particle goes from \mathbf{x} to \mathbf{y} , is given by the sum over all paths $\mathbf{x}(t)$ of the functional

$$\exp\left(i\int_{t'}^{t''} L[\mathbf{x}(t)]dt\right) \langle m | \exp\left(-i\int_{t'}^{t''} H'(t)dt\right) | n \rangle,$$

where the sum is taken only over paths such that $\mathbf{x}(t') = \mathbf{x}$ and $\mathbf{x}(t'') = \mathbf{y}$. This sum is denoted by

$$\int_{\substack{\mathbf{x}(t')=\mathbf{x} \\ \mathbf{x}(t'')=\mathbf{y}}} \mathfrak{D}\mathbf{x}(t).$$

H' depends on the path $\mathbf{x}(t)$ through the forcing function g . For any particular path, however, the matrix element is given by (9'). Hence, if we save the sum over paths and the integration on \mathbf{x} and \mathbf{y} till the end, the oscillator sums in (6') can be carried out as before, and we obtain²¹

$$f(\eta) = \left(\frac{a^2 \hbar k_i}{m}\right) NS(q) \int d(\mathbf{y}-\mathbf{x}) \exp[i\mathbf{q} \cdot (\mathbf{x}-\mathbf{y})] \\ \times \int_{\substack{\mathbf{x}(0)=\mathbf{x} \\ \mathbf{x}(\eta)=\mathbf{y}}} \mathfrak{D}\mathbf{x}(t) \exp\left(i\int_0^\eta L[\mathbf{x}(t)]dt\right) \\ \times \exp\{-\gamma A[\mathbf{x}(t)]\}, \quad (13')$$

where

$$A[\mathbf{x}(t)] = \int d\mathbf{k} \int_0^\eta \int_0^\eta dt ds \left[e^{i\mathbf{k} \cdot (\mathbf{x}_t - \mathbf{x}_s)} e^{-i\omega(t-s)} \right. \\ \left. \times \left(1 + \frac{1}{e^{\beta\omega} - 1} \right) + e^{-i\mathbf{k} \cdot (\mathbf{x}_t - \mathbf{x}_s)} \frac{e^{i\omega(t-s)}}{e^{\beta\omega} - 1} \right], \quad (14') \\ \gamma = \left(\frac{\partial \Delta}{\partial \rho}\right)^2 \left(\frac{\rho_0 \hbar}{2c}\right) \left(\frac{1}{(2\pi)^3}\right), \quad \omega = \hbar ck.$$

The Hamiltonian $\Delta + (p - p_0)^2/2\mu$ comes from the Lagrangian $L = -\Delta + \frac{1}{2}\mu |d\mathbf{x}/dt|^2 + |d\mathbf{x}/dt| p_0$. As $\mu \rightarrow \infty$, L becomes very large for all paths except the one with $d\mathbf{x}/dt = 0$. Consequently the main contribution to (13') comes from paths whose end points \mathbf{x} and \mathbf{y} are very close to each other; furthermore, the entire path must stay close to \mathbf{x} and \mathbf{y} . If μ is actually infinite, $\mathbf{x}_t - \mathbf{x}_s$ may be set equal to zero in (14'), and then (13') reduces to (11'), which we henceforth call $f_\infty(\eta)$. The actual value of μ is large; consequently, only for large η can the paths stray far enough from the origin to make $f(\eta)$ appreciably different from $f_\infty(\eta)$. Hence the line form is the same as that previously computed, except near the line center.

²¹ We have replaced \mathbf{q} by $-\mathbf{q}$. This clearly does not affect $f(\eta)$.

For any functional $M[\mathbf{x}(t)]$, we define

$$\langle M \rangle = \exp[iE(q)\eta] \int d(\mathbf{y}-\mathbf{x}) \exp[i\mathbf{q} \cdot (\mathbf{x}-\mathbf{y})] \\ \times \int_{\substack{\mathbf{x}(0)=\mathbf{x} \\ \mathbf{x}(\eta)=\mathbf{y}}} \mathfrak{D}\mathbf{x}(t) M[\mathbf{x}(t)] \exp\left(i\int_0^\eta L[\mathbf{x}(t)]dt\right).$$

The amplitude for a free particle to go from \mathbf{x} to \mathbf{y} in time η is

$$K_0(\mathbf{x}, \mathbf{y}, \eta) = \int_{\substack{\mathbf{x}(0)=\mathbf{x} \\ \mathbf{x}(\eta)=\mathbf{y}}} \mathfrak{D}\mathbf{x}(t) \exp\left(i\int_0^\eta L[\mathbf{x}(t)]dt\right) \\ = (2\pi)^{-3} \int d\mathbf{k} \exp\{i[\mathbf{k} \cdot (\mathbf{y}-\mathbf{x}) - E(k)\eta]\}, \quad (15')$$

and therefore $\langle 1 \rangle = 1$. The operation $\langle \rangle$, may be regarded as a kind of average. We want to find

$$\exp[-iE(q)\eta] \langle \exp(-\gamma A) \rangle.$$

If we define $\langle \exp(-\gamma A) \rangle = \exp(-\varphi)$, then φ can be expanded as a power series in γ :

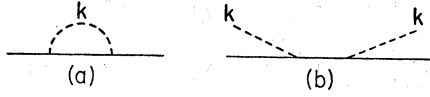
$$\varphi = \gamma \varphi_1 + \gamma^2 \varphi_2 + \dots,$$

where

$$\varphi_1 = \langle A \rangle, \quad -\varphi_2 = \frac{1}{2}(\langle A^2 \rangle - \langle A \rangle^2), \quad \text{etc.} \quad (16')$$

If the integrations on \mathbf{k} , t , and s are postponed, then the kind of integral which must be done in evaluating $\langle A \rangle$ is

$$I = \int d(\mathbf{y}-\mathbf{x}) e^{i\mathbf{q} \cdot (\mathbf{x}-\mathbf{y})} \int_{\substack{\mathbf{x}(0)=\mathbf{x} \\ \mathbf{x}(\eta)=\mathbf{y}}} \mathfrak{D}\mathbf{x}(t) e^{i\mathbf{k} \cdot (\mathbf{x}_t - \mathbf{x}_s)} e^{-i\omega(t-s)} \\ \times \exp\left(i\int_0^\eta L[\mathbf{x}(\tau)]d\tau\right) \\ = e^{-i\omega(t-s)} \int \int \int dy dx_2 dx_1 e^{-i\mathbf{q} \cdot \mathbf{y}} \\ \times \int_{\substack{\mathbf{x}(t)=\mathbf{x}_2 \\ \mathbf{x}(\eta)=\mathbf{y}}} \mathfrak{D}\mathbf{x}(\tau) \exp\left(i\int_t^\eta Ld\tau\right) e^{i\mathbf{k} \cdot \mathbf{x}_2} \\ \times \int_{\substack{\mathbf{x}(s)=\mathbf{x}_1 \\ \mathbf{x}(t)=\mathbf{x}_2}} \mathfrak{D}\mathbf{x}(\tau) \exp\left(i\int_s^t Ld\tau\right) e^{-i\mathbf{k} \cdot \mathbf{x}_1} \\ \times \int_{\substack{\mathbf{x}(0)=\mathbf{x} \\ \mathbf{x}(s)=\mathbf{x}_1}} \mathfrak{D}\mathbf{x}(\tau) \exp\left(i\int_0^s Ld\tau\right) e^{i\mathbf{q} \cdot \mathbf{x}} \\ = \int \int \int d(\mathbf{y}-\mathbf{x}_2) d(\mathbf{x}_2 - \mathbf{x}_1) d(\mathbf{x}_1 - \mathbf{x}) e^{-i\mathbf{q} \cdot (\mathbf{y}-\mathbf{x}_2)} \\ \times K_0(\mathbf{y}, \mathbf{x}_2, \eta - t) e^{-i\omega(t-s)} e^{-i(\mathbf{q}-\mathbf{k}) \cdot (\mathbf{x}_2 - \mathbf{x}_1)} \\ \times K_0(\mathbf{x}_2, \mathbf{x}_1, t - s) e^{-i\mathbf{q} \cdot (\mathbf{x}_1 - \mathbf{x})} K_0(\mathbf{x}_1, \mathbf{x}, s) \\ = \exp\{-i[E(\mathbf{q})(\eta - t) \\ + (E(\mathbf{q}-\mathbf{k}) + \omega)(t - s) + E(\mathbf{q})s]\}.$$

FIG. 10. Diagrams representing the two terms in $\langle A \rangle$.

This integral clearly describes the emission and re-absorption of a phonon of momentum $\hbar\mathbf{k}$ [Fig. 10(a)]. The second term in A , corresponding to absorption and re-emission [Fig. 10(b)], results in the integral

$$I' = \exp\{-i[E(\mathbf{q})(\eta-t) + (E(\mathbf{q}+\mathbf{k})-\omega)(t-s) + E(\mathbf{q})s]\}.$$

Similarly, $\langle A^2 \rangle$ gives rise to terms involving two phonons. To calculate $\langle A^n \rangle$, one must evaluate integrals of the form

$$J_\nu = \int_{0 < t_1 < t_2 < \dots < t_\nu < \eta} \dots \int dt_1 \dots dt_\nu \exp(i \sum \alpha_i t_i).$$

Defining new variables $x_1 = t_1$, $x_2 = t_2 - t_1$, \dots , $x_\nu = t_\nu - t_{\nu-1}$, and introducing the function

$$f(y) = \begin{cases} 1, & 0 < y < \eta \\ 0, & y > \eta \end{cases}$$

$$= \frac{i}{2\pi} \int_{-\infty}^{\infty} \left(\frac{e^{-is\eta} - 1}{s} \right) e^{isy} ds,$$

$$-\gamma \langle A \rangle = -\gamma \int d\mathbf{k} \, k \left[\left(1 + \frac{1}{e^{\beta\omega} - 1} \right) \left(\frac{i\eta}{E(\mathbf{q}) - E(\mathbf{q}-\mathbf{k}) - \omega} - \frac{e^{i[E(\mathbf{q}) - E(\mathbf{q}-\mathbf{k}) - \omega]\eta} - 1}{[E(\mathbf{q}) - E(\mathbf{q}-\mathbf{k}) - \omega]^2} \right) \right. \\ \left. + \frac{1}{e^{\beta\omega} - 1} \left(\frac{i\eta}{E(\mathbf{q}) - E(\mathbf{q}+\mathbf{k}) + \omega} - \frac{e^{i[E(\mathbf{q}) - E(\mathbf{q}+\mathbf{k}) + \omega]\eta} - 1}{[E(\mathbf{q}) - E(\mathbf{q}+\mathbf{k}) + \omega]^2} \right) \right]. \quad (18')$$

In the limit of infinite roton mass, (18') is the same as the exponent in (11'). This is to be expected, since if there is only one possible path, then $\langle \exp(-\gamma A) \rangle = \exp(-\gamma \langle A \rangle)$. The various terms in (18') have the same significance as in (11'), and agree with the results of perturbation theory. None of the denominators in (18') can vanish, since the roton is defined as the lowest state of momentum \mathbf{q} . If we approximate $\langle \exp(-\gamma A) \rangle$ by $\exp(-\gamma \langle A \rangle)$ in our evaluation of $f(\eta)$, then the delta function in $n(E)$ still persists.

One naturally thinks of going further with the series (16') and replacing $\langle \exp(-\gamma A) \rangle$ by $\exp[-(\gamma \langle A \rangle + \gamma^2 \varphi_2)]$. This procedure is not obviously valid, however, since we are interested in $f(\eta)$ for large η . Suppose, for instance, that φ_2 is linear in η for large η ,

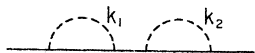


FIG. 11. A diagram which contributes a term to $\langle A^2 \rangle$ proportional to η^2 . This term is canceled by the square of (10a).

we find

$$J_\nu = \int_0^\infty \dots \int_0^\infty f(\sum x_i) \exp(i \sum \beta_i x_i) dx_1 \dots dx_\nu$$

$$= \frac{i}{2\pi} \int_{-\infty}^{\infty} ds \frac{e^{-is\eta} - 1}{s} \int_0^\infty \dots \int_0^\infty \exp[i \sum (\beta_i + s) x_i] dx_1 \dots dx_\nu$$

$$= \frac{1}{2\pi i^{\nu-1}} \int_{-\infty}^{\infty} ds \left[\left(\frac{e^{-is\eta} - 1}{s} \right) \prod_{i=1}^{\nu} \left(\frac{1}{\beta_i + s + i\epsilon_i} \right) \right].$$

$$(\beta_i = \sum_{j=i}^{\nu} \alpha_j)$$

To make the next to last integral converge, we have added a small positive imaginary part $i\epsilon_i$ to each β_i . All the ϵ_i will be taken as different, so that all poles are simple, even if some of the β_i are equal. Closing the contour in the lower half-plane, we have finally

$$J_\nu = \frac{1}{i^{\nu-2}} \sum \left[\left(\frac{e^{i(\beta_i - \epsilon_i)\eta} - 1}{\beta_i + i\epsilon_i} \right) \prod_{i \neq i} \left(\frac{1}{\beta_j - \beta_i + i(\epsilon_j - \epsilon_i)} \right) \right]. \quad (17')$$

The integral resulting from I has the form J_2 , with $\beta_1 = 0$, $\beta_2 = E(\mathbf{q}) - E(\mathbf{q}-\mathbf{k}) - \omega$. In general, the β_i are the energy differences between the initial state and various intermediate states. The time integral of I' is similarly evaluated, and we find

but some subsequent term in the series (16') involves higher powers of η . Then neglect of the subsequent terms would make $f(\eta)$ entirely incorrect for large η . However, by inspection of the diagrams which contribute to φ_n , it is quite easy to see that φ_n is always linear in η for large η . For instance, the "bubble" in Fig. 10(a) contributes a term to $\langle A \rangle$ proportional to η because it can occur anywhere on the solid line. Among the processes contributing to $\langle A^2 \rangle$ is the one shown in Fig. 11. Since each of the bubbles can occur (almost) anywhere on the solid line, Fig. 11 contributes a term proportional to η^2 ; but since the two bubbles are independent if the separation between them is large, the square of (10a) cancels the term in η^2 . There is a correction term in $\langle A^2 \rangle$ proportional to η because the two bubbles may overlap. Hence φ_2 is linear in η ; similar arguments apply to φ_n . Another way to see that φ is asymptotically linear in η is to observe that

for large η_1 and η_2 , $f(\eta)$ obeys the functional equation $f(\eta_1+\eta_2) \cong \text{const} \times f(\eta_1)f(\eta_2)$. We omit the proof.

The only part of $\gamma^2\varphi_2$ which interests us is the part proportional to η , since the rest is negligible compared with $\gamma\varphi_1$. Furthermore, pieces of $\gamma^2\varphi_2$ proportional to $i\eta$ represent small corrections to the self-energy and can be omitted. Hence we are interested only in the piece of φ_2 (if any) which is proportional to η with a real coefficient. Such a piece would cause attenuation of $f(\eta)$ for large η , and would imply that the delta function is gone.

The diagrams of Fig. 12 (and no others in this order) contribute the kind of terms we are looking for. For (12a) we have $\beta_1=0$, $\beta_2=\beta_4=E(\mathbf{q})+\omega_1-E(\mathbf{q}+\mathbf{k}_1)$, $\beta_3=E(\mathbf{q})+\omega_1-E(\mathbf{q}+\mathbf{k}_1-\mathbf{k}_2)-\omega_2$, and

$$-J_4(12a) = \frac{e^{-\epsilon_1\eta}-1}{i\epsilon_1} \left(\frac{1}{\beta_2^2(\beta_3+i\epsilon_3-i\epsilon_1)} \right) \\ + \frac{e^{i(\beta_3-\epsilon_3)\eta}-1}{\beta_3+i\epsilon_3} \left(\frac{1}{-\beta_3+i\epsilon_1-i\epsilon_3} \right) \left(\frac{1}{(\beta_2-\beta_3)^2} \right) + \dots,$$

where the dots indicate that uninteresting terms have been omitted. It is possible for β_3 to vanish; in fact the condition $\beta_3=0$ states that phonon-roton scattering is energetically possible. Since $1/(z+i\epsilon) = P(1/z) - i\pi\delta(z)$, the first term becomes²²

$$\frac{i\eta}{\beta_2^2} \left\{ P\left(\frac{1}{\beta_3}\right) + i\pi\delta(\beta_3) \right\}.$$

The principal value term is a correction to the self-energy and is omitted. Omitting uninteresting terms again, we find for the second term

$$\frac{\cos(\beta_3\eta)-1+i\sin(\beta_3\eta)}{\beta_3(\beta_2-\beta_3)^2} \left[-P\left(\frac{1}{\beta_3}\right) - i\pi\delta(\beta_3) \right] \\ = -\frac{\pi\eta}{\beta_2^2} \delta(\beta_3) + \frac{\pi\eta}{\beta_2^2} \delta(\beta_3) + \dots = 0 + \dots.$$

The net contribution of (12a) is

$$J_4(12a) = \frac{\pi\eta}{\beta_2^2} \delta(\beta_3) + \dots.$$

The contribution of (12b) has the same form, with $\beta_2=E(\mathbf{q})-E(\mathbf{q}-\mathbf{k}_1)-\omega_1$, $\beta_3=E(\mathbf{q})+\omega_2-E(\mathbf{q}-\mathbf{k}_1+\mathbf{k}_2)-\omega_1$. Similarly, (12c) contributes a term $(\pi\eta/\beta_2\beta_4)\delta(\beta_3)$, with $\beta_2=E(\mathbf{q})+\omega_1-E(\mathbf{q}+\mathbf{k}_1)$, $\beta_3=E(\mathbf{q})+\omega_1-E(\mathbf{q}+\mathbf{k}_1-\mathbf{k}_2)-\omega_2$, $\beta_4=E(\mathbf{q})-E(\mathbf{q}-\mathbf{k}_2)-\omega_2$; (12d) contributes

²² We are free to let ϵ_1 and ϵ_3 approach zero in any order, so long as we are consistent. We let $\epsilon_3 \rightarrow 0$ first.

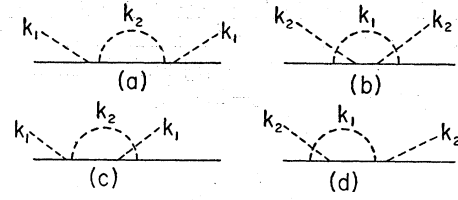


FIG. 12. Diagrams contributing attenuation to $f(\eta)$.

the same type of term, with

$$\beta_2 = E(\mathbf{q}) - E(\mathbf{q} - \mathbf{k}_1) - \omega_1, \\ \beta_3 = E(\mathbf{q}) + \omega_2 - E(\mathbf{q} + \mathbf{k}_2 - \mathbf{k}_1) - \omega_1, \\ \beta_4 = E(\mathbf{q}) + \omega_2 - E(\mathbf{q} + \mathbf{k}_2).$$

For fixed \mathbf{k}_1 and \mathbf{k}_2 we add the contributions of diagrams (12a)-(12d) to the contributions of the corresponding diagrams with \mathbf{k}_1 and \mathbf{k}_2 exchanged. Noting that $\delta(\beta_3) = -\delta(-\beta_3)$, we find

$$-\gamma^2\varphi_2 = \frac{1}{2}\gamma^2(\langle A^2 \rangle - \langle A \rangle^2) \\ = -\eta\gamma^2\pi \int \int d\mathbf{k}_1 d\mathbf{k}_2 k_1 k_2 \left(\frac{1}{e^{\beta\omega_1}-1} \right) \\ \times \left(\frac{1}{e^{\beta\omega_2}-1} + 1 \right) \left[\frac{1}{E(\mathbf{q}) + \omega_1 - E(\mathbf{q} + \mathbf{k}_1)} \right. \\ \left. + \frac{1}{E(\mathbf{q}) - \omega_2 - E(\mathbf{q} - \mathbf{k}_2)} \right]^2 \\ \times \delta[E(\mathbf{q} + \mathbf{k}_1 - \mathbf{k}_2) + \omega_2 - E(\mathbf{q}) - \omega_1] \\ = -\eta\hbar R/2,$$

where R is just the rate of roton-phonon scattering (Fig. 8) as computed in perturbation theory. Finally we find

$$f(\eta) \simeq (a^2\hbar k_i/m) NS(q) \exp[-(i\Delta\eta + \gamma\langle A \rangle + \eta\hbar R/2)] \\ \simeq f_\infty(\eta) \exp(-\eta\hbar R/2). \quad (19')$$

The only appreciable change in the line shape $n(E)$ is the replacement of the delta function by

$$\frac{1}{2\pi} \left(\frac{\hbar R}{(E - \Delta')^2 + \hbar^2 R^2/4} \right), \quad (20')$$

where Δ' is the corrected roton energy. The uncertainty principle is evidently satisfied.

As we remarked earlier, the real interaction between phonons and rotons is more complicated than the one we assumed. The line width is determined by the lifetime for roton-roton collisions, rather than roton-phonon collisions. Landau and Khalatnikov¹⁴ fitted the viscosity data by assuming a roton-roton interaction of the form $V_0\delta(\mathbf{r}_1-\mathbf{r}_2)$ with $V_0=0.5 \times 10^{-38}$ erg-cm³. The interaction term in (1'), which we call H' , allows one roton to emit a phonon which is absorbed by another roton.

In computing the equivalent potential, it is permissible to regard the rotons as distinguishable. If the initial state is $\psi_i = \exp[i(\mathbf{k}_1 \cdot \mathbf{r}_1 + \mathbf{k}_2 \cdot \mathbf{r}_2)]$ and the final state is $\psi_f = \exp\{i[(\mathbf{k}_1 + \mathbf{k}) \cdot \mathbf{r}_1 + (\mathbf{k}_2 - \mathbf{k}) \cdot \mathbf{r}_2]\}$, then the amplitude to go from i to f is

$$\sum_I \frac{H'_{if} H'_{Ii}}{E_I - E_i} = V_{\mathbf{k}}.$$

Roton 2 can emit a phonon \mathbf{k} which is then absorbed by 1, or roton 1 can emit a phonon $-\mathbf{k}$ which is then absorbed by 2. Neglecting the dependence of roton energy on the momentum, we find $V_{\mathbf{k}} = (\partial\Delta/\partial\rho)^2(\rho_0/c^2)$. The equivalent potential is $\sum V_{\mathbf{k}} e^{i\mathbf{k} \cdot \mathbf{r}_{12}} = (\partial\Delta/\partial\rho)^2(\rho_0/c^2) \times \delta(\mathbf{r}_{12})$ (actually, the delta function is smeared out by the high-momentum cutoff). Using the value of Atkins and Edwards¹⁵ for $\partial\Delta/\partial\rho$, we find $V_0 = 0.66 \times 10^{-38}$ erg-cm³. The $\mathbf{p} \cdot \mathbf{v}$ coupling between rotons and phonons (see next paragraph) gives rise to a velocity-dependent roton-roton interaction which seems comparable in strength to the one we have computed. If the picture of a roton as a moving smoke ring is correct, then the interaction between rotons would depend strongly on their relative orientations. Accordingly, even though the delta-function interaction can be simply explained, we think the actual roton-roton interaction is more complicated.

The interaction between phonons and rotons has been discussed by Landau and Khalatnikov, and

involves other terms besides $(\partial\Delta/\partial\rho)(\rho - \rho_0)$. A phonon induces a velocity field $\mathbf{v}(\mathbf{r})$ which can be represented in terms of the $a_{\mathbf{k}}$ and $a_{\mathbf{k}}^*$. In the presence of such a field, the energy of a roton of momentum \mathbf{p} is $E(\mathbf{p}) + \mathbf{p} \cdot \mathbf{v}$. Furthermore, there are terms in $(\rho - \rho_0)^2$, such as $(\partial^2\Delta/\partial\rho^2)(\rho - \rho_0)^2$, which are responsible for most of the phonon-roton scattering. Nevertheless, a line arising from roton production will still have the shape pictured in Fig. 8, provided the delta function is replaced by a "witch" of the form (20'), where R is the rate of roton-roton scattering. As the temperature approaches zero, the rate R approaches zero because no other excitations are present to scatter the roton. Furthermore, at $T=0$, $n(E)$ is "one sided" because it is impossible to produce an excitation of momentum \mathbf{q} with less energy than a roton. The curve hits the axis with finite slope because the rate of production of rotons, plus a phonon of frequency of ω , is proportional to ω for small ω . At finite temperatures, the background curve intersects the "witch" with finite slope on the right, and zero slope on the left,²³ because the rate of phonon production is proportional to $\omega[1 + (e^{\beta\omega} - 1)^{-1}]$ while the annihilation rate is proportional to $\omega(e^{\beta\omega} - 1)^{-1}$. All these statements depend only on the fact that the coupling is a power series in the $a_{\mathbf{k}}$ and $a_{\mathbf{k}}^*$, with each creation or destruction operator accompanied by a factor $k^{\frac{1}{2}}$.

²³ This is not exactly true. Processes involving several phonons can give rise to a small finite slope on the left.